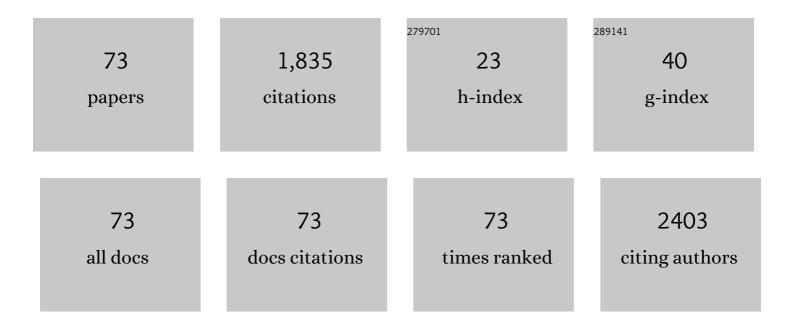
List of Publications by Year in descending order

Source: https://exaly.com/author-pdf/1706324/publications.pdf Version: 2024-02-01



#	Article	IF	CITATIONS
1	Four new indole alkaloids from the roots of <i>Isatis tinctoria</i> . Natural Product Research, 2022, 36, 312-318.	1.0	4
2	Explore the effect of LLYâ€283 on the ototoxicity of auditory cells caused by cisplatin: A bioinformatic analysis based on RNAâ€seq. Journal of Clinical Laboratory Analysis, 2022, 36, e24176.	0.9	3
3	Iridoids and lignans from Valeriana officinalis L. and their cytotoxic activities. Phytochemistry Letters, 2022, 49, 125-130.	0.6	0
4	Steroidal components from the roots and rhizomes of Helleborus thibetanus. Phytochemistry Letters, 2022, 50, 31-35.	0.6	2
5	<i>Sinomenium acutum</i> : A Comprehensive Review of its Botany, Phytochemistry, Pharmacology and Clinical Application. The American Journal of Chinese Medicine, 2022, 50, 1219-1253.	1.5	8
6	Vandetanib drives growth arrest and promotes sensitivity to imatinib in chronic myeloid leukemia by targeting ephrin <scp>typeâ€B</scp> receptor 4. Molecular Oncology, 2022, 16, 2747-2765.	2.1	4
7	Picraquanines Aï¼€, three new phenolic derivatives from the stems of Picrasma quassioides. Natural Product Research, 2021, 35, 3687-3693.	1.0	4
8	Indole alkaloid glycosides from <i>Isatis tinctoria</i> roots. Natural Product Research, 2021, 35, 244-250.	1.0	16
9	Inhibitors of BRD4 protein from the roots of Astilbe grandis stapf ex E.H. Wilson. Natural Product Research, 2021, 35, 2044-2050.	1.0	10
10	Three new steroidal components from the roots of <i>reineckia carnea</i> . Natural Product Research, 2021, 35, 1159-1166.	1.0	5
11	Isatisindigoticanine A, a novel indole alkaloid with an unpresented carbon skeleton from the roots of <i>Isatis tinctoria</i> . Natural Product Research, 2021, 35, 1249-1255.	1.0	12
12	Sanguinarine impedes metastasis and causes inversion of epithelial to mesenchymal transition in breast cancer. Phytomedicine, 2021, 84, 153500.	2.3	20
13	WWOX activation by toosendanin suppresses hepatocellular carcinoma metastasis through JAK2/Stat3 and Wnt/β-catenin signaling. Cancer Letters, 2021, 513, 50-62.	3.2	24
14	Selenium sulfide disrupts the PLAGL2/Câ€MET/STAT3â€induced resistance against mitochondrial apoptosis in hepatocellular carcinoma. Clinical and Translational Medicine, 2021, 11, e536.	1.7	13
15	<i>Schisandra sphenanthera</i> : A Comprehensive Review of its Botany, Phytochemistry, Pharmacology, and Clinical Applications. The American Journal of Chinese Medicine, 2021, 49, 1577-1622.	1.5	20
16	Design, synthesis and biological evaluation of novel thiazole-derivatives as mitochondrial targeting inhibitors of cancer cells. Bioorganic Chemistry, 2021, 114, 105015.	2.0	2
17	Overoxidized poly(3,4-ethylenedioxythiophene)–gold nanoparticles–graphene-modified electrode for the simultaneous detection of dopamine and uric acid in the presence of ascorbic acid. Journal of Pharmaceutical Analysis, 2021, 11, 699-708.	2.4	23
18	Dibenzocyclooctadiene lignans from the root bark of Schisandra sphenanthera. Phytochemistry Letters, 2021, 45, 137-141.	0.6	7

#	Article	IF	CITATIONS
19	Pregnane alkaloids with BRD4 inhibitory and cytotoxic activities from Pachysandra terminalis. Phytochemistry Letters, 2021, 45, 63-67.	0.6	4
20	Design, synthesis and antitumor activities of thiazole-containing mitochondrial targeting agents. Bioorganic Chemistry, 2021, 115, 105271.	2.0	3
21	Webâ€based transcriptome analysis determines a sixteenâ€gene signature and associated drugs on hearing loss patients: A bioinformatics approach. Journal of Clinical Laboratory Analysis, 2021, 35, e24065.	0.9	6
22	Electrodeposited poly(3,4-ethylenedioxythiophene) doped with graphene oxide for the simultaneous voltammetric determination of ascorbic acid, dopamine and uric acid. Mikrochimica Acta, 2020, 187, 94.	2.5	44
23	TPD7 inhibits the growth of cutaneous T cell lymphoma H9 cell through regulating ILâ€2R signalling pathway. Journal of Cellular and Molecular Medicine, 2020, 24, 984-995.	1.6	6
24	Three new indole alkaloid glycosides with unusual structural features from the roots of Isatis indigotica. Phytochemistry Letters, 2020, 39, 168-172.	0.6	7
25	Quassinoids and alkaloids from the stems of Picrasma quassioides with nitric oxide inhibitory activity. Phytochemistry Letters, 2020, 39, 68-72.	0.6	7
26	Synthesis and biological evaluation of geniposide derivatives as potent and selective PTPlB inhibitors. European Journal of Medicinal Chemistry, 2020, 205, 112508.	2.6	9
27	Layered Sulfur Nanosheets Prepared by Assembly of Sulfur Quantum Dots: Implications for Wide Optical Absorption and Multiwavelength Photoluminescence. ACS Applied Nano Materials, 2020, 3, 10749-10756.	2.4	22
28	Stable Layered Sulfur Nanosheets Prepared by One-Step Liquid-Phase Exfoliation of Natural Sublimed Sulfur with Bovine Serum Albumin for Photocatalysis. Chemistry of Materials, 2020, 32, 10476-10481.	3.2	18
29	A novel anthracene derivative with an asymmetric structure as an electron transport material for stable Rec. 2020 blue organic light-emitting diodes. Journal of Information Display, 2020, 21, 197-201.	2.1	5
30	Cantharidin treatment inhibits hepatocellular carcinoma development by regulating the JAK2/STAT3 and PI3K/Akt pathways in an EphB4-dependent manner. Pharmacological Research, 2020, 158, 104868.	3.1	34
31	Bisindole alkaloids with nitric oxide inhibitory activities from an alcohol extract of the Isatis indigotica roots. Fìtoterapìâ, 2020, 146, 104654.	1.1	9
32	Four undescribed sulfur-containing indole alkaloids with nitric oxide inhibitory activities from Isatis tinctoria L. roots. Phytochemistry, 2020, 174, 112337.	1.4	23
33	Sanguinarine disrupts the colocalization and interaction of HIFâ€1α with tyrosine and serine phosphorylated TAT3 in breast cancer. Journal of Cellular and Molecular Medicine, 2020, 24, 3756-3761.	1.6	20
34	Chemical constituents isolated from the roots and rhizomes of Smilacina japonica. Biochemical Systematics and Ecology, 2019, 86, 103920.	0.6	0
35	Alkaloid Enantiomers from the Roots of Isatis indigotica. Molecules, 2019, 24, 3140.	1.7	15
36	Direct electrochemistry of glucose oxidase based on one step electrodeposition of reduced graphene oxide incorporating polymerized l-lysine and its application in glucose sensing. Materials Science and Engineering C, 2019, 104, 109880.	3.8	27

#	Article	IF	CITATIONS
37	Lignans from Isatis indigotica roots and their inhibitory effects on nitric oxide production. FA¬toterapA¬A¢, 2019, 137, 104189.	1.1	24
38	Preparation of a glassy carbon electrode modified with reduced graphene oxide and overoxidized electropolymerized polypyrrole, and its application to the determination of dopamine in the presence of ascorbic acid and uric acid. Mikrochimica Acta, 2019, 186, 407.	2.5	32
39	Anti-diabetic potential of Pueraria lobata root extract through promoting insulin signaling by PTP1B inhibition. Bioorganic Chemistry, 2019, 87, 12-15.	2.0	20
40	Alkaloids with Nitric Oxide Inhibitory Activities from the Roots of Isatis tinctoria. Molecules, 2019, 24, 4033.	1.7	23
41	Sanguinarine inhibits epithelial–mesenchymal transition via targeting HIF-1α/TGF-β feed-forward loop in hepatocellular carcinoma. Cell Death and Disease, 2019, 10, 939.	2.7	57
42	Ephrin type-B receptor 4 affinity chromatography: An effective and rapid method studying the active compounds targeting Ephrin type-B receptor 4. Journal of Chromatography A, 2019, 1586, 82-90.	1.8	12
43	HMQâ€Tâ€F2 exert antitumour effects by upregulation of Axin in human cervical HeLa cells. Journal of Cellular and Molecular Medicine, 2018, 22, 2955-2959.	1.6	5
44	Steroidal Constituents from Roots and Rhizomes of Smilacina japonica. Molecules, 2018, 23, 798.	1.7	14
45	Novel compounds TAD-1822-7-F2 and F5 inhibited HeLa cells growth through the JAK/Stat signaling pathway. Biomedicine and Pharmacotherapy, 2018, 103, 118-126.	2.5	10
46	Berberine inhibits the proliferation and migration of breast cancer ZR-75-30 cells by targeting Ephrin-B2. Phytomedicine, 2017, 25, 45-51.	2.3	62
47	Dihydroberberine exhibits synergistic effects with sunitinib on NSCLC NCIâ€H460 cells by repressing MAP kinase pathways and inflammatory mediators. Journal of Cellular and Molecular Medicine, 2017, 21, 2573-2585.	1.6	7
48	Antiproliferative activity and SARs of caffeic acid esters with mono-substituted phenylethanols moiety. Bioorganic and Medicinal Chemistry Letters, 2017, 27, 131-134.	1.0	26
49	DNA–affibody nanoparticles for inhibiting breast cancer cells overexpressing HER2. Chemical Communications, 2017, 53, 573-576.	2.2	34
50	Electrodeposited reduced graphene oxide incorporating polymerization of l-lysine on electrode surface and its application in simultaneous electrochemical determination of ascorbic acid, dopamine and uric acid. Materials Science and Engineering C, 2017, 70, 241-249.	3.8	91
51	Two new pregnane glycosides from Reineckia carnea. Phytochemistry Letters, 2016, 15, 142-146.	0.6	22
52	Real-time amperometric monitoring of cellular hydrogen peroxide based on electrodeposited reduced graphene oxide incorporating adsorption of electroactive methylene blue hybrid composites. Journal of Electroanalytical Chemistry, 2016, 780, 60-67.	1.9	18
53	Characterization of Interactions Between Taspine Derivate TPD7 and EGF Receptor by Cell Membrane Chromatography with Zonal Elution and Frontal Analysis. Chromatographia, 2016, 79, 1585-1592.	0.7	4
54	Voltammetric Determination of Folic Acid Using Adsorption of Methylene Blue onto Electrodeposited of Reduced Graphene Oxide Film Modified Glassy Carbon Electrode. Electroanalysis, 2016, 28, 312-319.	1.5	44

#	Article	IF	CITATIONS
55	Electrochemical Behavior and Voltammetric Determination of Curcumin at Electrochemically Reduced Graphene Oxide Modified Glassy Carbon Electrode. Electroanalysis, 2016, 28, 749-756.	1.5	45
56	A novel tissue model for angiogenesis: evaluation of inhibitors or promoters in tissue level. Scientific Reports, 2015, 4, 3693.	1.6	8
57	Interactions between histamine H1 receptor and its antagonists by using cell membrane chromatography method. Journal of Pharmacy and Pharmacology, 2015, 67, 1567-1574.	1.2	8
58	Steroidal Saponins from the Roots and Rhizomes of Tupistra chinensis. Molecules, 2015, 20, 13659-13669.	1.7	24
59	Two new spirostanol saponins from the the roots and rhizomes of Tupistra chinensis. Phytochemistry Letters, 2015, 13, 6-10.	0.6	18
60	Steroidal glycosides from Reineckia carnea. Fìtoterapìâ, 2015, 105, 240-245.	1.1	27
61	Potential roles of Centipede Scolopendra extracts as a strategy against EGFR-dependent cancers. American Journal of Translational Research (discontinued), 2015, 7, 39-52.	0.0	12
62	c-Myc plays a key role in TADs-induced apoptosis and cell cycle arrest in human hepatocellular carcinoma cells. American Journal of Cancer Research, 2015, 5, 1076-88.	1.4	3
63	Simultaneous voltammetric determination of ascorbic acid and uric acid using a seven-hole carbon nanotube paste multielectrode array. Analytical Methods, 2014, 6, 8965-8972.	1.3	15
64	Eupolyphaga sinensis Walker displays inhibition on hepatocellular carcinoma through regulating cell growth and metastasis signaling. Scientific Reports, 2014, 4, 5518.	1.6	24
65	Brucine suppresses colon cancer cells growth <i>via</i> mediating <scp>KDR</scp> signalling pathway. Journal of Cellular and Molecular Medicine, 2013, 17, 1316-1324.	1.6	20
66	Graphene oxide/poly-l-lysine assembled layer for adhesion and electrochemical impedance detection of leukemia K562 cancercells. Biosensors and Bioelectronics, 2013, 42, 112-118.	5.3	107
67	Sensitive Voltammetric Determination of Baicalein at Thermally Reduced Graphene Oxide Modified Glassy Carbon Electrode. Electroanalysis, 2013, 25, 2136-2144.	1.5	34
68	Preparation, characterization, and application of electrochemically functional graphene nanocomposites by one-step liquid-phase exfoliation of natural flake graphite with methylene blue. Nano Research, 2012, 5, 875-887.	5.8	38
69	Electrochemically functional graphene nanostructure and layer-by-layer nanocomposite incorporating adsorption of electroactive methylene blue. Electrochimica Acta, 2012, 75, 71-79.	2.6	35
70	Label-free electrochemical DNA biosensor array for simultaneous detection of the HIV-1 and HIV-2 oligonucleotides incorporating different hairpin-DNA probes and redox indicator. Biosensors and Bioelectronics, 2010, 25, 1088-1094.	5.3	124
71	Application of multielectrode array modified with carbon nanotubes to simultaneous amperometric determination of dihydroxybenzene isomers. Sensors and Actuators B: Chemical, 2009, 136, 113-121.	4.0	114
72	Label-free and sensitive faradic impedance aptasensor for the determination of lysozyme based on target-induced aptamer displacement. Biosensors and Bioelectronics, 2009, 25, 94-99.	5.3	90

#	Article	IF	CITATIONS
73	Electrochemical impedance spectroscopy for study of aptamer–thrombin interfacial interactions. Biosensors and Bioelectronics, 2008, 23, 1624-1630.	5.3	148